JOURNAL OF MATERIALS SCIENCE 18 (1983) 1315–1322

Electrical behaviour of doped-yttria stabilized zirconia ceramic materials

C. PASCUAL*, J. R. JURADO, P. DURAN
Instituto de Cerámica y Vidrio, CSIC, Arganda del Rey, Madrid, Spain

Single-phase sintered ceramic materials $(ZrO_2)_{1-x}\{(Y_2O_3)_y(RE_2O_3)_{1-y}\}_x$ (RE=Nd, Ce, Dy, Er), were synthesized and electrical conductivity and transport number measurements were made as a function of temperature between 500 and 1200° C. The activation energies of conduction were determined, and it was found that the charge carriers in these solid solutions are oxygen ions. The fabricated electrolyte discs were used in cells of the type P_{O_2}, Pt/zirconia solid solution/P'_{O_2}, platinum where P_{O_2} = air (0.21 atm) and P'_{O_2} = 1 atm or argon–O_2 mixtures. Below 700° C, the e.m.f. deviated from the theoretical values for completely ionic conduction; good agreement was observed above this temperature.

1. Introduction

In recent years a considerable number of works have been devoted to the study of ZrO_2 as a solid electrolyte. Pure zirconia cannot be used as a solid electrolyte due to the disruptive monoclinic–tetragonal transformation at about 1200° C. By the addition of some metal oxides (mainly MgO, CaO, Y_2O_3 and rare earth oxides), the transformation can be suppressed and monoclinic zirconia can be stabilized in a cubic form with an oxygen-deficient fluorite lattice. The anionic defects lead to high ionic conduction at high temperatures.

The ionic conduction in doped zirconia has been reported by several authors [1–3], and it is at present generally assumed that the solid electrolyte based on $(ZrO_2)_{0.91}(Y_2O_3)_{0.09}$ is better than solid electrolytes based on zirconia stabilized with MgO or CaO, which decompose to monoclinic zirconia after prolonged heating at low temperature. The identification of the ideal composition $(ZrO_2)_{0.91}(Y_2O_3)_{0.09}$ is based on previous studies by Dixon *et al.* [4] and Strickler and Carlson [5] who found that a maximum for the ionic conductivity was present at the fluorite phase boundary ($\simeq 9$ mol% Y_2O_3). Recently, Stubican *et al.* [6] and Pascual and Duran [7] have reported that the existence of an eutectoid decomposition of this solid solution at low temperature (400 to 500° C) is possible. Such eutectoid decomposition would have a deleterious effect on the electrical behaviour of the above solid solution.

It is known that the ionic conduction is due to the migration of O^{2-} ions through vacant ion sites when the Zr^{4+} ions are partially replaced by dopant ions having a valence less than 4 +. Beyond the maximum ($\simeq 9$ mol% Y_2O_3), the ionic conduction is strongly diminished by the increasing of the vacancy concentration, because of the limitation of the oxygen-ion mobility. Then, if the vacancy concentration is kept constant (about 4% for the case of the $(ZrO_2)_{0.91}(Y_2O_3)_{0.09}$ solid solution), the maximum conductivity also could be obtained by stabilizing the zirconia with others ions and, if the addition has certain crystallographic results, the formation of a solid solution more stable than that would be possible.

The present work is devoted to the study of the electrical behaviour of Y_2O_3 and YRE_2O_3-stabilized zirconia specimens from the point of view of its possible application as an oxygen sensor, on the basis of the results of X-ray diffraction, stability, microstructure, electrical conductivity and transport-number measurements.

*This work is based on the PhD thesis of C. Pascual, Madrid University (1980).

0022–2461/83 $03.00 + .12

2. Experimental procedure

2.1. Specimens preparation

The starting materials used were of 99.9% purity. Mixtures of ZrO_2 with Y_2O_3 or Y_2O_3 + RE oxides (RE=Ce, Nd, Dy, Er) were made in such ratios that the composition corresponded to $(ZrO_2)_{1-x}(Y_2O_3)_x$ or $(ZrO_2)_{1-x}(YRE_2O_3)_x$, where x varied between 0.09 to 0.14. Batches of 100 g of material were carefully weighed and wet blended in pure acetone for 60 min. After being calcined at 1500° C for 2 h, the samples were ball-milled for 4 h with alumina balls. The particle size of the powders was always $<35\mu$. The samples used for the electrical measurements were obtained by isostatic pressing the powders at about 20.000 psi*, and by sintering at 1800° C for 8 h in a gas furnace.

2.2. Sample characterization

The phases present in the sintered specimens were studied by means of X-ray diffraction in which Cu$K\alpha$ radiation was used. The scanning speed was 2θ min^{-1} = 1/2° min^{-1}. For the determination of the lattice constants, the high angle lines (3 3 1) and (4 0 2) were used. The accuracy of the calculated lattice parameters was ± 0.005 nm.

As an additional check on the possible presence of a second phase, the microstructure of samples was examined by light-reflected microscope and SEM (scanning electron microscopy). The samples were polished and adequately etched to reveal the grain boundaries.

2.3. Electrical conductivity

The total electrical conductivity of the samples was measured in air at 50° C intervals, from 500 to 1150° C. Platinum foil electrodes were incorporated on to the samples during pressing and their dimensions were 40 mm x 5 mm x 5 mm after sintering. Samples were held by platinum wires, welded to the electrodes, and suspended in the hot zone of the furnace. The sample temperature was monitored by a Pallador thermocouple placed near the sample. During each measurement, the temperature was constant to within ± 2° C. Currents employed ranged from 5×10^{-6} to 2×10^{-2} A, and the potential across the samples varied between 2 and 2.3 V. A four terminal a.c. technique was used to measure the conductivity (see Fig. 1a). A current was passed through the sample and the potential drop across the two centre leads was measured with a high impedance voltmeter. In some cases, two-point a.c. measurements at 1592 Hz were made with a Wayne–Kerr Model B221A universal bridge, and similar results were obtained by both methods. No measurements were made to check the frequency-dependence of the conductivity.

2.4. e.m.f. measurements

Transport-numbers were measured by the e.m.f. method. A vertical type gas flow apparatus was made, whose schematic profile is shown in Fig. 1b.

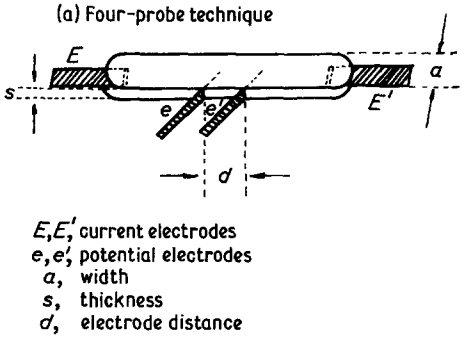

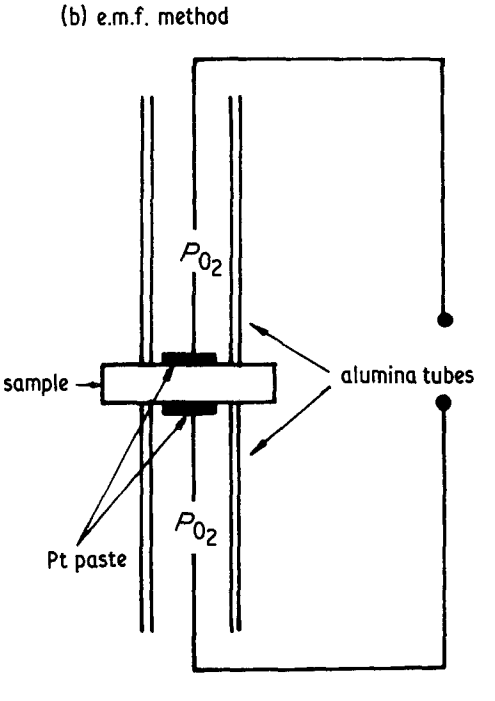

Figure 1 Schematic diagram of (a) *a–c* technique conductivity measurement, (b) transport-number measurement.

*1 psi = 6.89 × 10^3 Pa.

A 22 mm diameter and 3 mm thick disc sample was sandwiched between platinum packings to which alumina tubes were attached. The platinum packings, which soften at high temperatures, ensure the gas tightness of the cell. In addition, a spring force placed at the upper end of the alumina tube ensured the gas tightness. The sample disc was coated on both sides with platinum paste and made contact with platinum mesh attached to 0.35 mm platinum wires that served as the two current leads. A pallador thermocouple was placed near the sample. To minimize thermoelectric potentials induced by a temperature gradient, the specimen was located at the thermal centre of the furnace. The accuracy of the temperature measurements was always better than $\pm 2^{\circ}$ C. Oxygen or argon–oxygen mixtures were introduced by means of an inner gas guide placed in the lower space. In this way, one side of the sample was exposed to air and the other side to pure oxygen or to the O_2–argon mixtures. In all cases the gas was passed at a total pressure of 1 atm and linear flow rates varying between 0.5 and 1.0 cm sec^{-1}. The gas was not preheated, but the attainment of equilibrium between the specimen and the surrounding atmosphere was assured by heating the sample in a given atmosphere for several hours at each temperature, before e.m.f. measurement were made.

Gas mixtures were chosen at high oxygen pressures ranging from 1 to 10^{-5} atm, and these were achieved by using O_2–argon mixtures. Thus, the response of the solid electrolyte was determined by changing the oxygen partial pressure from 0.21 atm (air) to 10^{-5} atm (O_2–argon mixture) as a function of temperature.

When the two sides of the sample disc are exposed to different oxygen partial pressures P_{O_2} and P'_{O_2}, an electromotive force is generated across the electrodes, given by the Nernst equation,

$$E_{obs} = (RT/4F)\,\bar{t}_i \ln (P_{O_2}/P'_{O_2}) \qquad (1)$$

where E_{obs} is the observed e.m.f. of the following cell

$$O_2(P'_{O_2}),\ Pt/\text{zirconia solid solution}/O_2(P_{O_2}),\ Pt$$

and where R and F are the gas and Faraday constants, respectively, T is the absolute temperature,

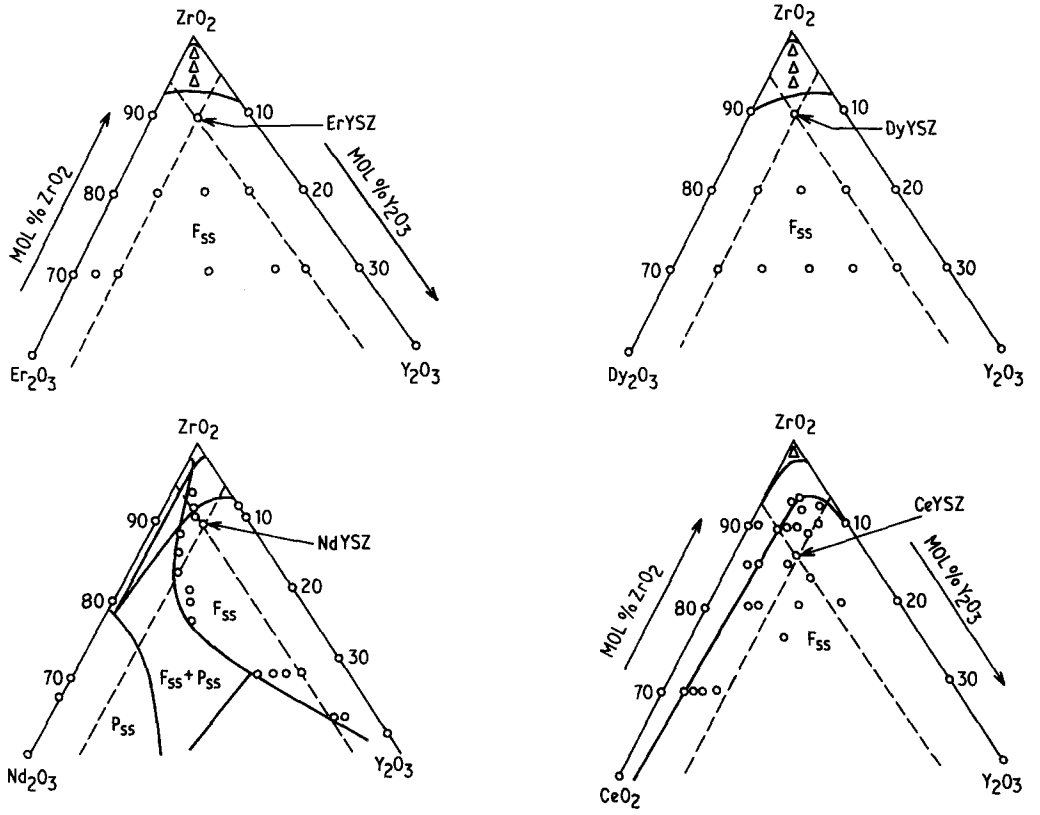

Figure 2 Ternary phase diagram in the fluorite-rich region for the ZrO_2–Y_2O_3–RE_2O_3 systems.

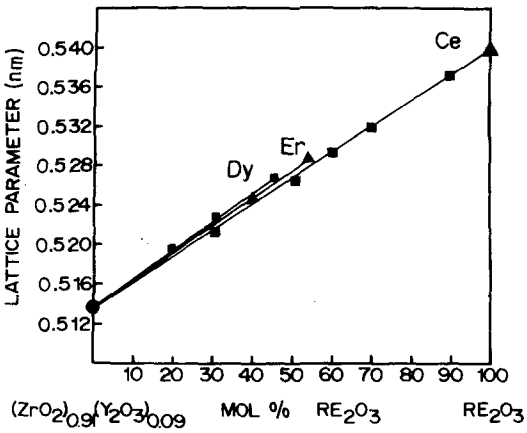

Figure 3 Room-temperature lattice parameters of $(ZrO_2)_{0.91}(Y_2O_3)_{0.09}$-$RE_2O_3$ compositions.

and $\bar{t}_i$ is the average oxygen ion transference number. When $\bar{t}_i = 1$, the theoretical e.m.f. can be obtained from the above expression; the E_{obs}/E_{th} ratio gives the true value of $\bar{t}_i$ for the zirconia solid solution sample. The output from the cell was monitored with a digital voltmeter with high input impedance.

3. Results and discussion

3.1. Fluorite solid solution domains and sample characterization

Although it was not a goal of the present work, a preliminary study of the fluorite solid solution domains was carried out for the ZrO_2–Y_2O_3–RE_2O_3 systems. Fig. 2 shows the partial phase diagram, in the tentative form for compositions which were heated at 1800° C for 8 h and slowly cooled to room temperature. On each system, the composition ZYRE studied has been represented. The compositions were selected taking into account that a maximum in the oxygen-ion conductivity occurs at 4.16% anion vacancies (between 9 and 10 mol% Y_2O_3) [4]. On this basis, compositions containing 10 mol% (Y_2O_3 + RE_2O_3) were chosen. The only exception was the case of the system ZrO_2–Y_2O_3–CeO_2, where the composition contained 14 mol% (Y_2O_3 + CeO_2), because of the different behaviour of the CeO_2 in the zirconia stabilization. Fig. 3 shows the lattice parameter variation for the fluorite solid solution in the various systems. From this result, an inter-

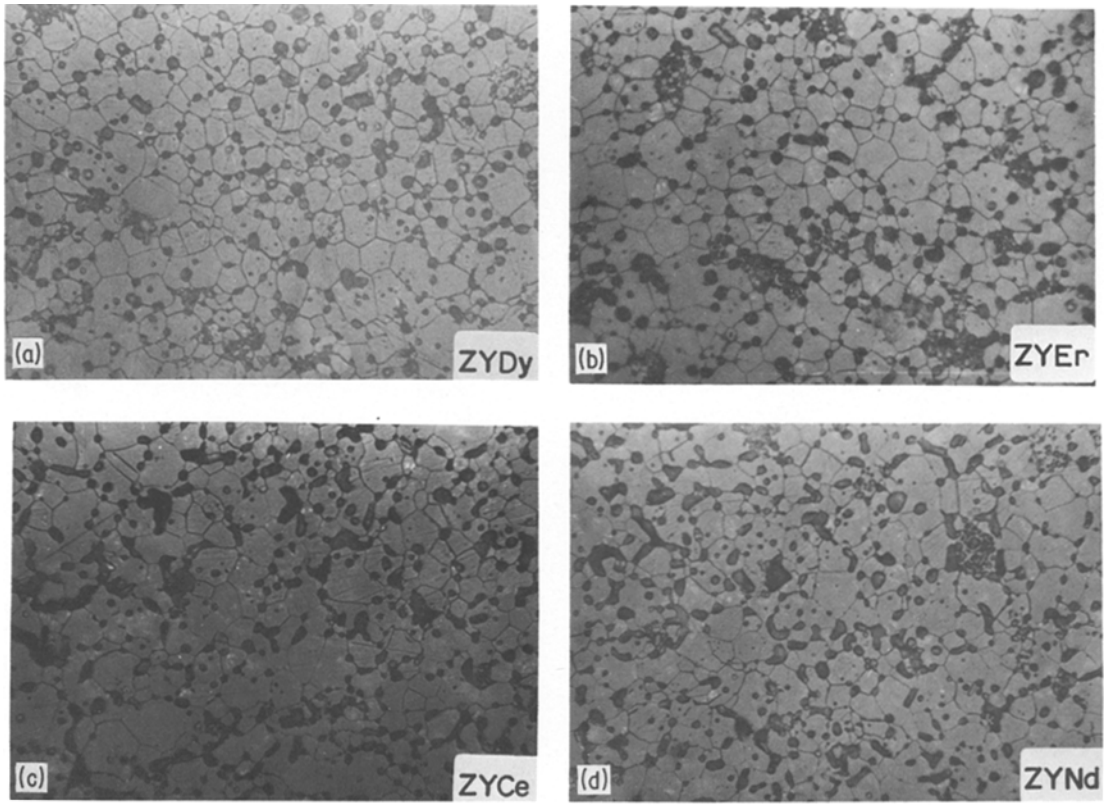

Figure 4 Typical microstructure of the doped-yttria stabilized zirconia compositions (480 ×). (a) ZYDy, (b) ZYEr, (c) ZYCe, and (d) ZYNd.

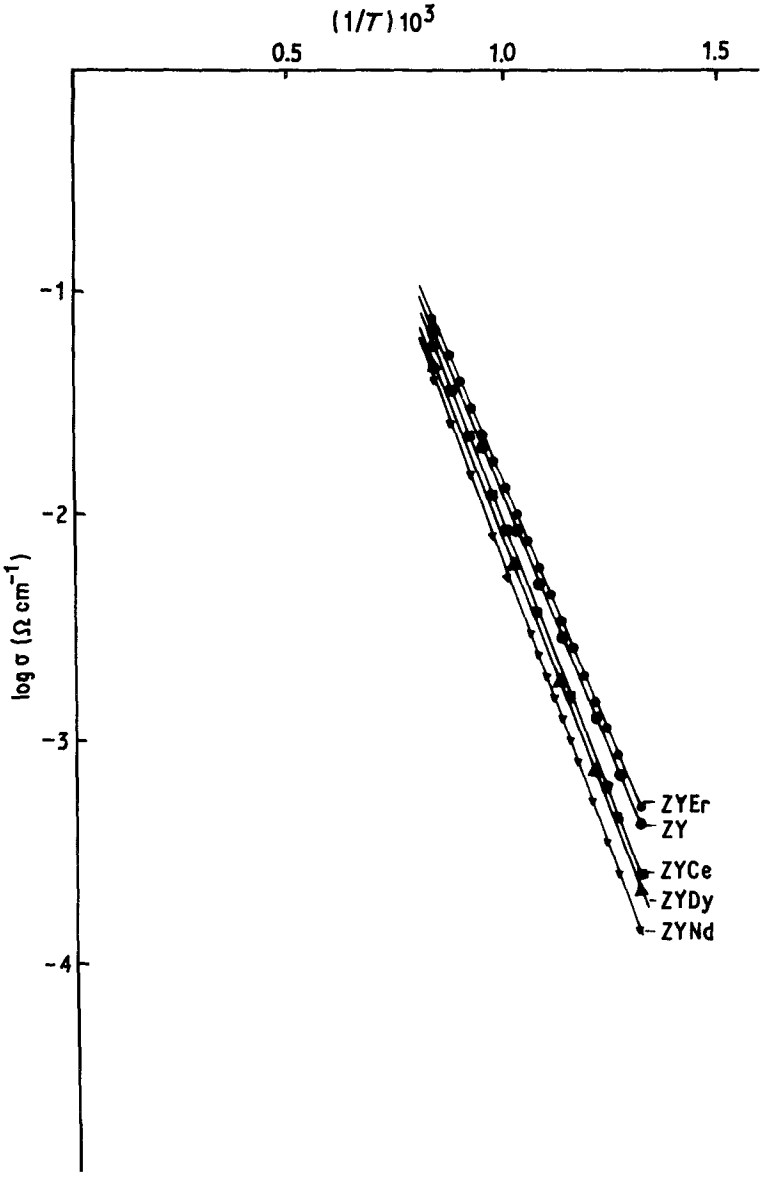

Figure 5 Arrhenius plot of total conductivity of the doped-yttria stabilized zironia compositions.

pretation of the solubility mechanism of the two additives in zirconia could be given. Primarily, the Y^{3+} substitutes for the Zr^{4+} ion in the lattice according to Kroeger–Vink [8] notation, as follows,

$$Y_2O_3 \rightarrow 2Y'_{Zr} + V_O^{\cdot\cdot} + 3O_0^x \qquad (2)$$

and the ratio between the anionic and cationic sites is maintained by creating an oxygen vacancy, $V_O^{\cdot\cdot}$, for each two Y^{3+} introduced.

On the other hand, the second dopant can enter the zirconia lattice in either of the two ways:

(a) $RE_2O_3 \rightarrow 2RE'_{Zr} + V_O^{\cdot\cdot} + 3O_0^x$

(b) $RE_2O_3 + 3V_O^{\cdot\cdot} \rightarrow 2RE_i^{\cdot\cdot\cdot} + 3O_0^x$

where RE'_{Zr} is a RE ion on a Zr^{4+} site and $V_O^{\cdot\cdot}$ an oxygen vacancy. $RE_i^{\cdot\cdot\cdot}$ is an interstitial RE ion. Because of the large increase in lattice constant measured versus dissolved RE_2O_3, in agreement with Vegard's law, we assumed that the RE enters the zirconia lattice substitutionally.

The density of the selected samples was always $\geqslant 90\%$ of the theoretical value. A previous study of the influence of porosity on the electrical conductivity [9] showed that no effect takes place when this is smaller than 15%. The microstructure of representative samples for $(ZrO_2)_{0.90}(Y_2O_3)_{0.05}(RE_2O_3)_{0.05}$ and $(ZrO_2)_{0.86}(YO)_{0.07}(CeO)_{0.07}$ compositions may be seen from Fig. 4. This examination confirms the single phase nature of the samples, in close agreement with

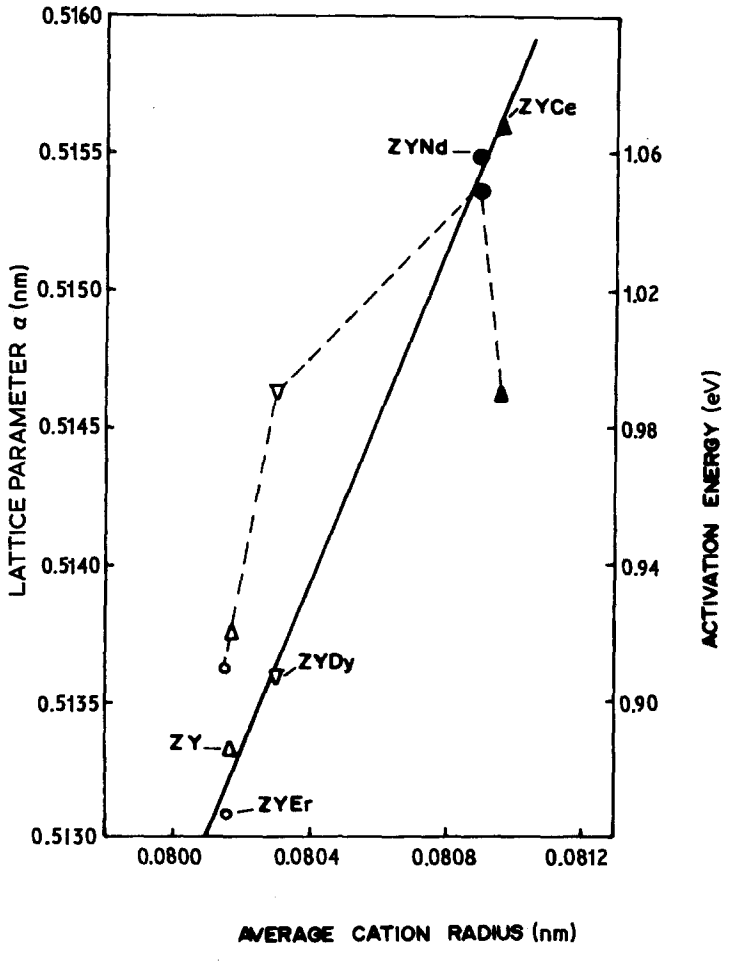

Figure 6 Lattice parameters and activation energy (dashed line) variation as a function of the average cation radius for the different ternary fluorite solid solutions.

the phase diagram studies. The thermal stability of these solid solutions was studied elsewhere [10], and no decomposition below 1200° C was observed.

3.2. Electrical conductivity

The results of the electrical conductivity measurements are shown in Fig. 5 for selected samples in air at 1600 Hz in the range 500 to 1150° C. It can be seen that a good linear log σ–$1/T$ relationship was present in all the cases, in agreement with the equation $\sigma = \sigma_0 \exp(-E_a/kT)$. One slope, and not two, is found. This result disagrees with those of Browal and Doremus [11] in which some changes in slope were found for different compositions in doped yttria-stabilized zirconias. This could be related with the different method used for the electrical conductivity measurements. It is well known now that electrode effects are present when the two-probe a.c. technique is used. With the four-probe a.c. technique we have eliminated this problem, and only a single slope was found throughout the temperature region in all the cases. Schouler *et al.* [12, 13] reported that even those measurements carried out at a fixed frequency can also be in error. Their results, however, could be considered as not conclusive, and we think that great care must be taken when interpreting the results obtained on ceramic samples from different methods and working conditions. A replotting of the data using log σT or log $\sigma T^{3/2}$ did not improve the linearity of the data, but the energy activation values increased.

From Fig. 6, it can be seen that the energy of activation increases with the average cation radius. Since the vacancy concentration is the same, except for the ZrO_2–Y_2O_3–CeO_2 composition, and if we assume that the activation energy is that required to move the oxygen ions through channels formed by neighbouring cations, then the oxygen diffusion rate could be controlled by the radius of these channels which is, on the other hand, a function of the average cation radius and the lattice parameter of the solid solutions.

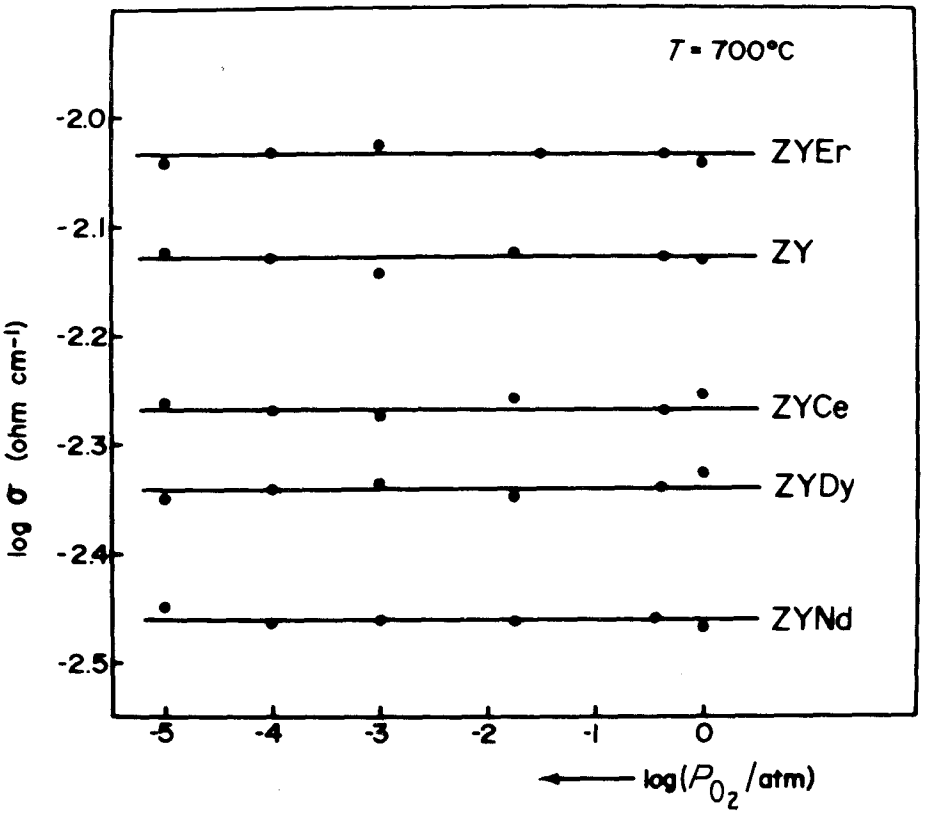

Figure 7 Total conductivity against oxygen partial pressure.

Since the geometry leads to an expression, $s = (a/6^{1/2}) - \bar{r}_c$ (where s is the radius of the channels, a the lattice parameter, and $\bar{r}_c$, the average cation radius), we have calculated the values of s for the different solid solutions, and have found that the activation energy for conduction is lower for those solid solutions in which s is larger, i.e. $Er^{3+} < Y^{3+} < Dy^{3+} < Ce^{4+} < Nd^{3+}$.

Although there are not many data from the literature to compare with the results obtained in the present work, it is clear that the cubic solid solution $(ZrO_2)_{0.91}(Y_2O_3)_{0.09}$ possesses the highest value for the electric conductivity among all the compositions studied. It should be mentioned, however, that for the ZYEr solid solution a higher electrical conductivity was found.

3.3. Oxygen ion transference number

In the range of the high oxygen partial pressures (1 to 10^{-5} atm), the electrical conductivity is essentially ionic (see Fig. 7), and the results of the transport-number measurements are shown in Fig. 8 as a function of temperature, between 500 and 1100° C. It can be seen that above 700° C, the agreement between the theoretical and experimental e.m.f. is very good. Below this temperature, the measured E values deviated from the theoretical e.m.f. for all the compositions. This non-ideal behaviour was also reported by Kudo and Obayashi [14] and Dirstine *et al.* [15] for the case of ceria–Ln_2O_3 and ceria–CaO solid solutions, respectively. At first, they attributed this anomalous behaviour to the irreversibility of the electrodes. However, Dirstine *et al.* [15] believe that the irreversible behaviour was due to the previous heat treatment of the paste electrode. In view of this result, we fired the platinum paste electrode in two different ways (*in situ* or previously sintered for 15 to 30 min at 750 to 800° C), and in both cases similar results were obtained. On the basis of our experimental results we believe that the non-ideal behaviour shown in Fig. 8 could be associated to nonequilibrium chemical reactions and, probably, electrochemical processes which occur on the sample electrodes. Franklin [16] and Brook *et al.* [17] also reported similar electrode effects on calcia-stabilized zirconia electrolytes.

Above that critical temperature (about 600° C), all the studied solid solutions showed a Nernstian

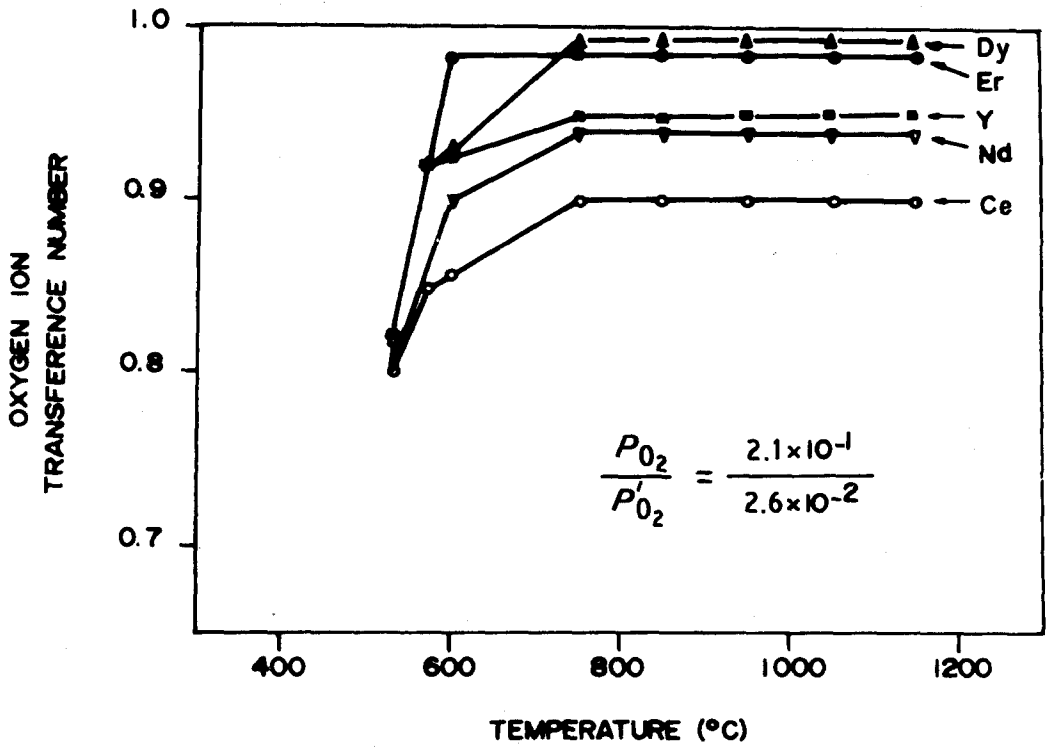

Figure 8 Transport-number against temperature for ternary fluorite compositions.

behaviour. The transference number for ZY and ZYNd saturates at 0.95 to 0.96, and these e.m.f. discrepancies are presumed to be due to a little larger porosities than the other compositions suggesting there are minor polarization effects associated with molecular or atomic transport through the electrolytes. For ZYCe solid solution which gives a lower transference number (about 0.90) this deviation could be related to reduction phenomena of the $Ce^{4+} \rightarrow Ce^{3+}$ type which, on the other hand, could influence the oxygen ion transport.

The response for the different solid solutions investigated here by cycling between high and low oxygen pressures was not studied, and this precludes the possibility of achieving a definite conclusion on the application possibilities of these materials. Other studies are in progress, in which a wider number of compositions and oxygen pressure ranges are expected to give a more satisfactory knowledge on the same.

References

1. K. KIUKOLA and J. WAGNER, *J. Electrochem. Soc.* 104 (1957) 79.
2. W. D. KINGERY, J. PAPPIS, M. E. DOTZ and D. C. HILL, *J. Amer. Ceram. Soc.* 42 (1959) 393.
3. C. B. ALCOCK and B. C. H. STTELE, *Sci. Ceram.* 2 (1965) 397.
4. J. DIXON, L. LAGRANGE, U. MERTEN, C. MILLER and J. PORTER, *J. Electrochem. Soc.* 110 (1963).
5. D. W. STRICKLER and W. G. CARLSON, *J. Amer. Ceram. Soc.* 47 (1964) 122.
6. V. S. STUBICAN, R. C. HINK and S. P. RAY, *J. Amer. Ceram. Soc.* 61 (1978) 17.
7. C. PASCUAL and P. DURAN, *J. Amer. Ceram. Soc.* 66 (1983).
8. F. A. KROEGER, *J. Amer. Ceram. Soc.* 49 (1966) 215.
9. C. PASCUAL, PhD thesis, Madrid (1980).
10. P. DURAN, *La Cerámica* 30 (1978) 7.
11. K. W. BROWAL and R. H. DOREMUS, *J. Amer. Ceram. Soc.* 60 (1977) 262.
12. E. SCHOULER, M. KLEITZ and C. DEPORTES, *J. Chim. Phys.* 70 (1973) 923.
13. E. SCHOULER, G. GIROUD and M. KLEITZ, *ibid.* 70 (1973) 1309.
14. T. KUDO and H. OBAYASHI, *J. Electrochem. Soc.* 122 (1975) 142.
15. R. T. DIRSTINE, W. O. GENTRY, R. N. BLUMENTHAL and W. HAMMETTER, *Amer. Ceram. Soc. Bull.* 58 (1979) 778.
16. A. D. FRANKLIN, *J. Amer. Ceram. Soc.* 58 (1975) 465.
17. R. J. BROOK, W. L. PELZMANN and F. A. KROEGER, *J. Electrochem. Soc.* 118 (1971) 185.

Received 1 June
and accepted 23 September 1982